Heliyon 10 (2024) e29195

Contents lists available at ScienceDirect

Heliyon

journal homepage: www.cell.com/heliyon

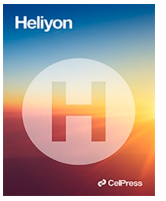

Research article

Response of heterologously expressed pressure sensor-actuator-modulator macromolecule to external mechanical stress

Subrata Batabyal, Chinenye Idigo, Darryl Narcisse, Adnan Dibas, Samarendra Mohanty *

Nanoscope Technologies LLC, 1312 Brown Trail, Bedford, TX, 76022, USA

ARTICLE INFO

Keywords:
Mechanosensitive channel
Osmoregulatory-channel
Pressure regulator

ABSTRACT

Cells from different organs in the body experience a range of mechanical and osmotic pressures that change in various diseases, including neurological, cardiovascular, ophthalmological, and renal diseases. Here, we demonstrate the use of an engineered Sensor-Actuator-Modulator (SAM) of microbial origin derived from a mechanosensitive channel of large conductance (MscL) for sensing external mechanical stress and modulating activities of mammalian cells. SAM is reliably expressed in the mammalian cell membrane and acts as a tension-activated pressure release valve. Further, the activities of heterologously expressed SAM in mammalian cells could be modulated by osmotic pressure. A comparison of the mechanosensitive activities of SAM-variants from different microbial origins shows differential inward current and dye uptake in response to mechanical stress exerted by hypo-osmotic shock. The use of SAM channels as mechanical stress-activated modulators in mammalian cells could provide new therapeutic approaches for treating disorders related to mechanical or osmotic pressure.

1. Introduction

Clogging of arteries or outflow pathways in the eyes and brain leads to arterial, intracranial, and ocular hypertension and related injury. In cases of hypertension, the blood exerts pressure against the walls of the blood vessels, which can lead to severe health complications and increase the risk of heart disease, stroke, and sometimes death. Cells from different organs in the body experience a range of mechanical and osmotic pressures that change in various diseases, including neurological, cardiovascular, ophthalmological, and renal diseases [1,2]. Although osmotic stress in renal diseases is well-known, many non-renal tissues routinely experience osmotic stress that can lead to disease initiation and progression but is often neglected[1]. Moreover, increasing evidence shows that osmotic stress triggers proinflammatory cytokine release and inflammation [3]. Osmotic stress causes oxidative stress that perturbs cell function and damages the DNA, resulting in cell cycle arrest and apoptosis [4].

While mechanosensitive channel [5–8] of large conductance (MscL) functions as an osmoregulator and protects bacteria cells from lysis upon hypo-osmotic shock, such channels are not present in mammalian cells. MscL directly senses tension in the membrane lipid bilayer of the swelling cell and, in response, transiently opens its large non-specific pore to release cytoplasmic fluid, thereby relieving the building turgor pressure [6,9–12]. The mechanosensitive channel of large conductance (MscL) is autonomous and does not need

* Corresponding author.
E-mail address: smohanty@nanoscopetech.com (S. Mohanty).

https://doi.org/10.1016/j.heliyon.2024.e29195
Received 21 December 2023; Received in revised form 29 March 2024; Accepted 2 April 2024
Available online 4 April 2024

partners or energy sources to function. MscL intrinsically senses tension in the membrane and gates in direct response to this mechanical tension. MscL is a relatively small homo-oligomeric channel that opens a large non-specific pore (~25-30 Å) to release water, ions, and macromolecules [13]' [5,12,14]. Other mechanosensitive channels from bacteria [15,16] (e.g., MscS, MscK, and MscG) and plant [17] (MSL2-10) also act as osmoregulators or diuretics [18].

We hypothesize that it may be possible to use the heterologously expressed mechanosensitive channels as a tension-activated pressure-release-valve in cells, including trabeculocytes, epithelial cells, and other cells of the body that are subjected to mechanical or osmotic pressure for therapeutic purposes. Such molecular shunts could provide an alternative outflow/inflow pathway for fluid in the treatment and prevention of edemas. However, different disease conditions, tissues, and associated pathophysiology would require the modulation of mechanical and/or osmotic pressure at different activation thresholds and to different degrees. Since mechanosensitive channels' activities are triggered solely by the transduction of mechanical force through lipid-protein interactions, amino acid residues that form those interfaces are critical for changing the activation threshold and mechanosensitivity of the channel [19]. For example, substituting the K101 residue of EcMscL for a negatively charged amino acid disrupts protein-lipid interactions, resulting in a channel that has longer open dwelling times and is less mechanosensitive than wild-type [20]. Likewise, the lipid composition of the host membrane greatly affects the properties of mechanosensitive channels. For example, in the *E. coli* membrane, *M. tuberculosis*-MscL is ~30% less mechanosensitive than in its native membrane [21].

Here, we demonstrate that MscL from multiple microbes is functional in mammalian cells, and the cells expressing MscL act as osmoregulators and activate mechanosensitive channels when subjected to osmotic pressure. Further, mutations to the residues of the mechanosensitive channel were found to adjust mechanosensitivity, including channel current. These results suggest that the microbial channel(s) would function in the foreign environment under a specific range of mechanical stimuli or osmotic stress generated inside the body or externally using a specific device.

2. Results

2.1. Design, cloning, and expression of Sensor-Actuator Modulator

High-resolution crystal structures[18] for mechanosensitive ion channels from bacteria *Mycobacterium tuberculosis* (MtMscL) are shown in Fig. 1A–C. Sequence homology analysis indicates *Escherichia coli* (EcMscL) shares 35% and 65% homology with MtMscL and Vibrio MscL respectively (Fig. 1D). These solved protein structures and homology comparisons allowed rational targeting of specific regions within the bacterial channels for mutagenesis engineering. Our goal was to customize the mechanosensitivity and modulate cellular responses to osmotic and mechanical forces (Fig. 1E). We optimized the bacterial channel codons for mammalian cell expression and engineered variants we term Sensor-Actuator Modulators (SAM). These engineered channels retain the innate sensation of membrane tension but with bespoke biophysical properties and cell-type-specific responses.

Fig. 2 shows the design, cloning, and expression of various SAM constructs derived from different bacteria and/or have undergone mutation. SAM1 consists of the *E. coli* MscL (EcMscL) gene (BL21(DE3) strain), which encodes for 136 amino acids, has codons

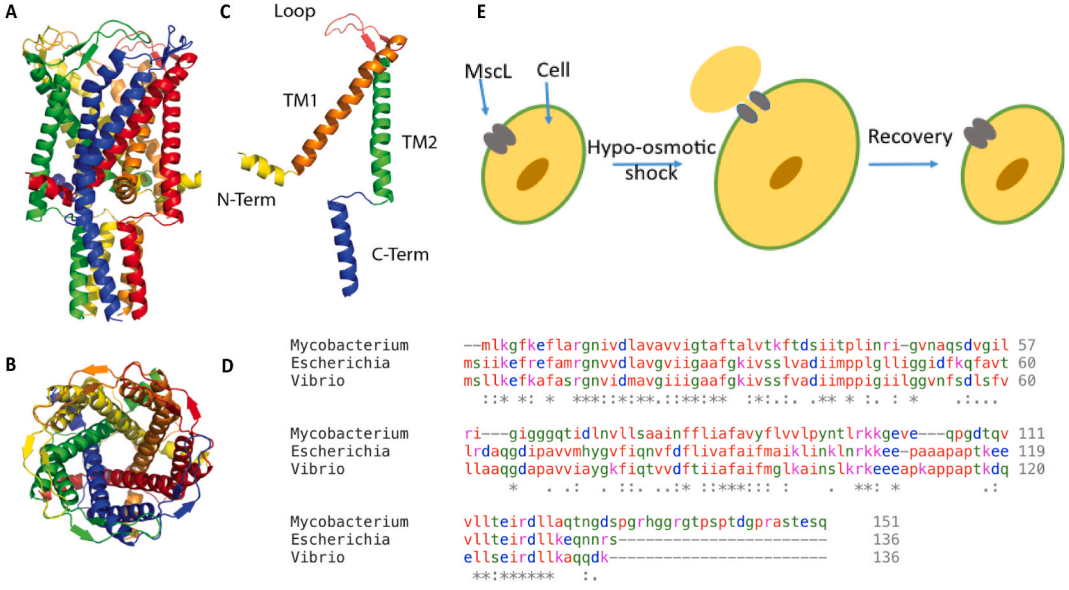

Fig. 1. Macromolecular Sensor, Actuator and Modulator (SAM). High-resolution crystal structure of Mt-MscL: (A) Lateral and (B) Top-down (PDB: 2OAR). (C) A monomer of Mt-MscL identifying secondary structure elements. (D) Homology alignment of Ec-, and Mt-MscL: EcMscL - MtMscL is 35%, VcMscL - MtMscL is 34%, EcMscL - VcMscL is 65%. (E) Principle of the response of cells sensitized with MscL to hypo-osmotic shock or external mechanical stress.

optimized for mammalian cell expression, and is C-terminally fused to mCherry (fluorescent reporter). SAM101 is the mutated version of SAM1 with point mutations (I113L/I70E) in the EcMscL sequence [22]. The other two SAM constructs, derived from *M. Tuberculosis* (SAM2) and *V. Cholera* (SAM3), also contained a ubiquitous promoter (CAG) (Fig. 2A). These designed SAM sequences were inserted into a cloning vector between two restriction sites, and the constructs were verified by sequencing and restriction digestion, followed by agarose electrophoresis (Fig. 2B; Supplementary Fig. 1, for SAM1). The expression of the SAM2 transgene was confirmed by transfection of HEK 293 cells (lipofection, JetPrime), followed by imaging of mCherry (reporter) fluorescence as shown in Fig. 2C. All constructs could be expressed in HEK cells, indicating that SAM can be expressed in mammalian hosts. To further verify the SAM expression, Western blot analysis of the lysate of HEK 293 cells transfected with SAM1 and SAM2 was carried out. The Western blot analysis revealed characteristic bands of SAM1 and SAM2 as shown in Fig. 2D (Supplementary Fig. 2), while the non-transfected HEK cells (-ve control, -SAM1) did not yield any band.

2.2. Functional characterization of SAM variants using hypo-osmotic down shock assay

In-vitro experiments were performed to demonstrate that bacterial mechanosensitive channels retain their native function in mammalian cells and can be used for molecular delivery and osmotic pressure control. To evaluate the hypothesis, HEK 293 cells were transfected with different SAM variants (Fig. 3) and were subjected to a hypo-osmotic shock (addition of 20% water v/v). The cells were monitored by confocal microscopy for ~10 min. Fig. 3 shows HEK 293 cells transfected with different SAM genes, subjected to a hypo-osmotic shock, in the presence of actin-binding Phalloidin (i.e., membrane-impermeable-molecule) by the addition of 20% water (v/v). The expression of SAM genes is shown in Fig. 3A and B. The kinetics of dye uptake in the cells were monitored using confocal fluorescence microscopy (Fig. 3C–E). Based on fluorescence kinetics measurement, it can be deduced that the increase in fluorescence is a function of SAM expression level, pore opening sizes, and opening probability. Thus, transfection with the SAM construct led to the expression of a functional membrane-integrated SAM channel protein capable of osmoregulation and molecular delivery. A bar graph comparison of the area under the curve of dye intake in different SAM channel-response to hypo-osmotic shock is shown in Fig. 3F. Among the three tested SAM variants, the SAM101 expressing cells led to the highest fluorescence intensity, implying a more efficient response to osmotic shock.

2.3. Viability of SAM-expressing cells under hypo-osmotic shock

While control (non-SAM transfected) HEK cells lost viability under a hypotonic (240 mOsm/kg) environment, cells expressing SAM could maintain viability in such stressed conditions, as measured by a high throughput, automated fluorescence microscope (NucleoCounter® NC-3000™). Fig. 3G shows the quantification of measured viability of HEK cells in isotonic (280 mOsm/kg) and hypotonic (240 mOsm/kg) environments, without and with SAM transfection. Further, a comparison of HEK cell diameter in isotonic (280 mOsm/kg) and hypotonic (240 mOsm/kg) environments, without and with EMC transfection, shows that the diameter of EMC-expressing cells did not increase in contrast to control cells (Fig. 3H).

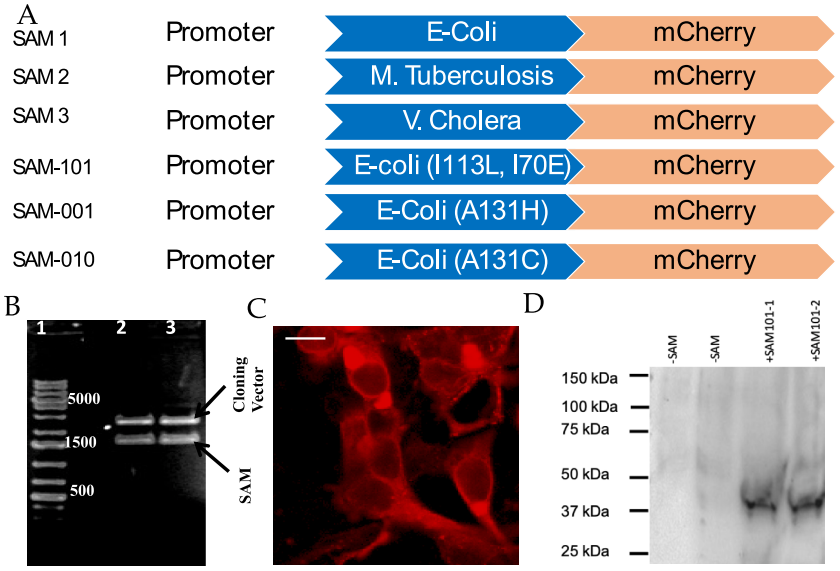

Fig. 2. Design, cloning, and expression of Sensor-Actuator Modulator (SAM) constructs in mammalian cells. (A) Typical domain architecture of SAM constructs with 5′ promoter sequences and 3′ fluorescent reporter sequences. (B) DNA agarose gel of restriction double digest products of SAM1 plasmid construct (Lanes 2,3), cloned between two restriction sites (BamHI and SalI), and DNA ladder (Lane 1). (C) Reporter (mCherry) fluorescence of SAM2 transfected HEK293 cells. Scale bar: 10 μm. (D) Western blot of HEK293 cells transfected with SAM101-mCherry plasmid. Lanes 1 and 2 (-SAM) are cells without plasmid. Lanes 3 and 4 (+SAM101-1 and +SAM101-2) are cells transfected with plasmid.

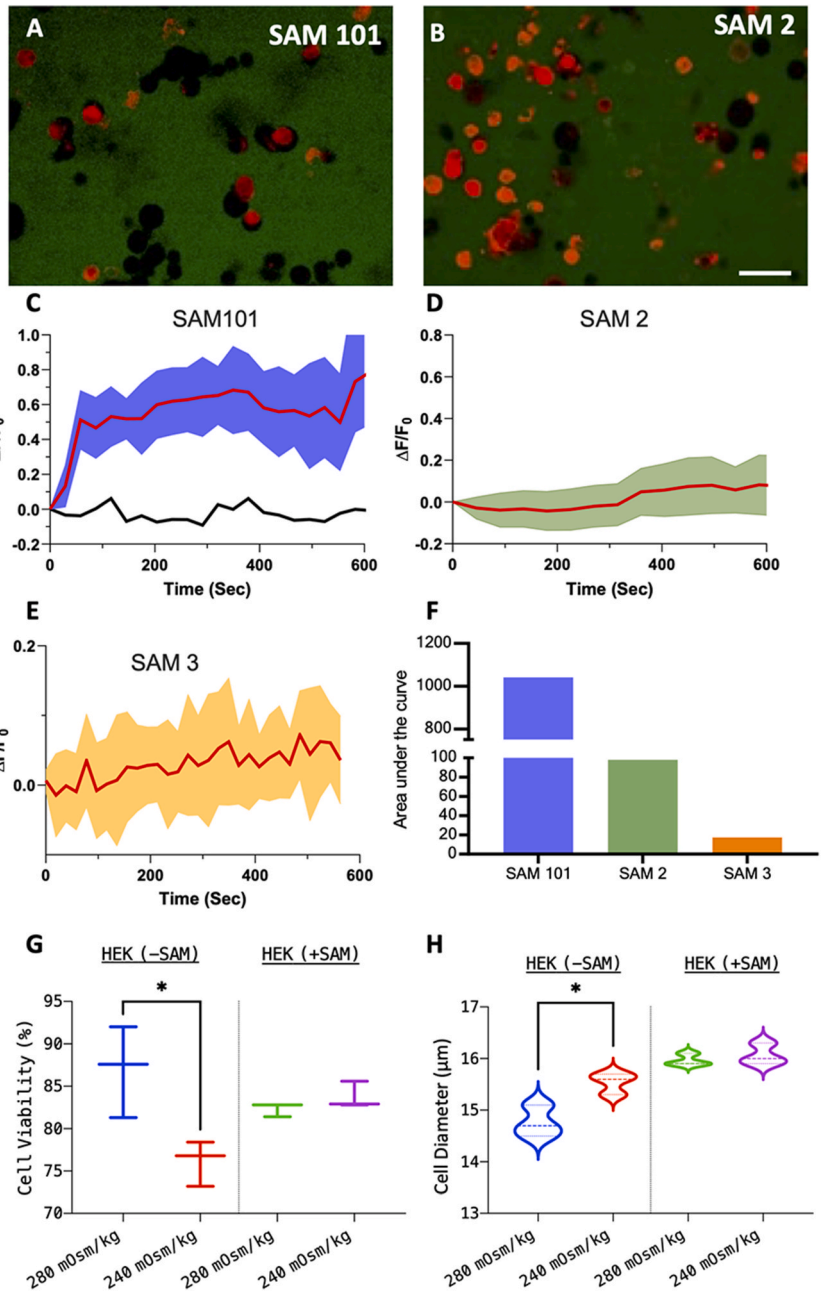

Fig. 3. Hypo-Osmotic Down Shock Assay confirms SAM channel-pore opening in HEK cells without compromising cell viability. (A–B) Confocal fluorescence image of HEK cells transfected with SAM-mCherry plasmids; Scale bar: 50 μm. The SAM-mCherry expressing cells are in red and non-expressing cells are in black (surrounded by green-fluorescent impermeable dye in the medium). (C–E) Kinetics of intensity of actin-bound fluorescence in SAM101, SAM2, and SAM3-transduced cells incubated with actin-staining Alexa Fluor™ 488 Phalloidin dye after a hypo-osmotic shock (addition of 20% v/v water). The shaded area represents the standard deviation around the mean (solid line). The black line represents the mean kinetics of fluorescence measured in -ve control (non-transfected) cells. (F) Quantitative comparison of membrane porosity (dye uptake, measured by area under fluorescence kinetic profile) for SAM variants. The bar graph shows the comparison area under the curve of intake of dye in different SAM channel responses to hypo-osmotic shock. (G) Quantification of measured viability of HEK cells in isotonic (280 mOsm/kg) and hypotonic (240 mOsm/kg) environments, without and with SAM transfection. (H) Comparison of HEK cell diameter in isotonic (280 mOsm/kg) and hypotonic (240 mOsm/kg) environments, without and with SAM transfection. $N > 10^5$ cells. (For interpretation of the references to colour in this figure legend, the reader is referred to the Web version of this article.)

2.4. Functional characterization of SAM in mammalian cells by electrophysiology

SAM channel function in mammalian cells was probed by recording electrophysiological measurements from whole cell patches of HEK 293 cells expressing different SAM variants. Channel activities were induced by subjecting the patched cell to a hypo-osmotic shock by adding 20% water (v/v) (Fig. 4A and B). Currents were measured while holding cells in a voltage clamp at −70 mV. A stable seal was achieved, and the current traces show channel activities only after the hypo-osmotic shock, as shown in Fig. 4C for the SAM2 variant. Upon hypo-osmotic shock, the SAM101-expressing cells exhibited spontaneous activity with a higher current as compared to SAM2. A quantitative comparison of different SAM-channel activities is shown in Fig. 4D, demonstrating that the SAM101 channel has higher activities than SAM1 and SAM2 in mammalian cells. Fig. 4E shows the quantitative comparison of SAM-101 activity measured using an automated pressure clamp (in HEK cells) compared to other mutants (SAM-001: A131H; SAM-010: A131C) as well as wildtype SAM.

3. Discussion

As reported in the literature, MscL channel upon expression in mammalian cells, allows the cells to be activated or modulated by external stimuli by mechanical force that causes stretch and deformation of the lipid bilayer, such as stretch, pressure/suction, and ultrasound [6,9,23]. Molecular delivery or transport has been reported by charge-induced activation [24] of *E. Coli* mechanosensitive channel (MscL) as well as by other modes of force transduction in mammalian cells [25]. Most studies have focused on MscL channel activation in mammalian cells requiring externally applied triggers/stimuli. In addition, the use of an external ultrasound stimulation device will further aid in molecular delivery, osmoregulation, stimulation [26,27], or cellular death (in the case of tumor) leading to the desired therapeutic outcome [23]. Here, we hypothesized that through protein engineering, the channel can be customized to autoregulate different pressure/osmotic changes in mammalian cells within pathological microenvironments.

In our study, we designed variants of MscL from different microbes (*E. coli, M. tuberculosis, VcMscL*) and we showed the functional expression of SAM (MscL) variants derived from three different microbes. A self-cleaving P2A peptide sequence was incorporated between the SAM channel coding region and a downstream mCherry fluorescent reporter gene within the expression vector. This enables stoichiometric co-expression of both the channel and reporter from a single transcript while allowing the translated proteins to diffuse independently following ribosomal cleavage of the peptide sequence. We observed that cells expressing SAM variants act as osmoregulators and generate inward currents when subjected to osmotic pressure. These results suggest that the microbial channel(s) would function in the foreign environment under a specific range of osmotic stress generated inside the body. Fluorescence images show that after a hypo-osmotic shock, the red fluorescent SAM-expressing cells did not swell significantly. This was confirmed by high throughput microscopic measurement of SAM-expressing cells under a hypo-osmotic environment. Further, mutations to the residues of the protein (*E. coli* SAM) were found to adjust mechanosensitivity, and channel kinetics (measured by patch clamp

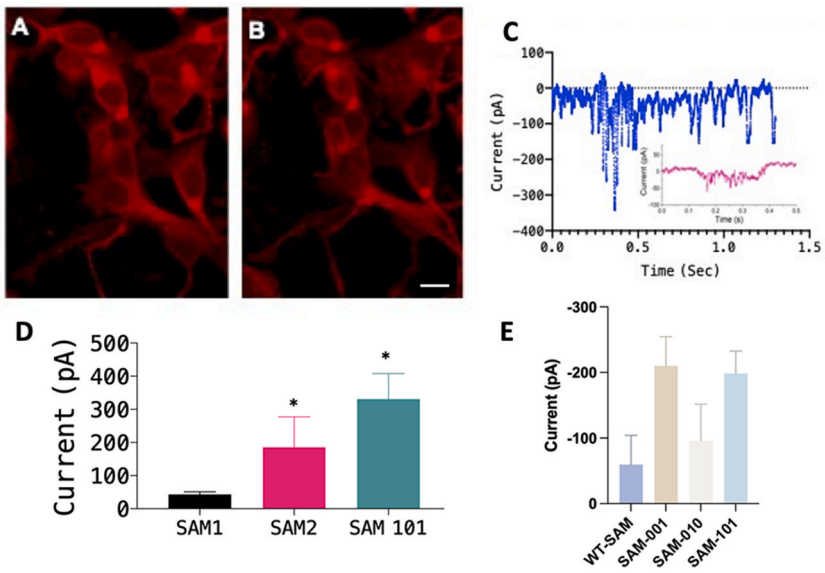

Fig. 4. Functioning of SAM-variants in mammalian cell confirmed by Patch clamp electrophysiology. (A) Membrane-specific expression in SAM-mCherry transfected HEK 293 cell, (B) Fluorescence image of SAM-expressing cells after the hypo-osmotic shock. Scale bar: 10 μm. (C) Current trace showing SAM2 channel activities after the hypo-osmotic shock. The inset trace shows the channel activities after the hypo-osmotic shock for SAM1. (D) A quantitative comparison of different SAM-Channel activity demonstrates that the SAM101 channel has higher activity than SAM1 and SAM2 in mammalian cells. N = 5 cells/condition. Av ± S.D. *$p < 0.05$ between SAM1 and others (SAM2 and SAM-101). (E) Quantitative comparison of SAM-101 activity measured using automated pressure clamp compared to wildtype SAM and other mutants (SAM-001: A131H; SAM-010: A131C).

electrophysiology). Activation of such heterologously expressed mechanosensitive channels in mammalian cells may allow tension-activated pressure release in the eye and arteries to reduce hypertension. These heterologously expressed mechanosensitive channels can be used as osmoregulators or diuretics, activated by internal mechanical stimuli, in the renal system in the treatment and prevention of kidney stones and chronic kidney diseases [28].

Further, these microbial mechanosensitive channels or their generated site-directed mutants can act as macromolecular pressure-release-valves, activated by internal or external mechanical stimuli, and an alternative outflow pathway for fluid in the treatment of idiopathic intracranial hypertension [29]. However, these mechanosensitive channels, their variants, and the generated site-directed mutants need to be activated at selected pressures, such as greater than 20 mmHg in the eye; or 120–200 mmHg (systolic) and 80–110 (diastolic) in the artery; or greater than 15 mmHg intracranial pressure. SAM variants, or generated site-directed mutants, can be delivered via viral or non-viral (physical, chemical, optical [30–33]) methods and can be expressed in targeted mammalian cells in a promoter-specific manner. However, the physiological translation of SAM-channel gating measured via *in-vitro* electrophysiology, may not exactly translate to pressure changes *in vivo*. In such a case, new SAM mutants may need to be engineered, or SAM-expressing cells can be activated externally. For efficient modulation of cells, targeting SAM to the cell membrane instead of cytosolic protein localization will be crucial. This can be achieved by using an optimal signal peptide.

The current study corroborates the hypothesis that the different microbial MscL can be engineered and expressed in mammalian cells and the engineered channels can enhance the innate sensation of membrane tension. Further, with molecular engineering, customized biophysical properties and cell-type-specific responses can be achieved by mutation of the channels. This would enable self-regulated, on-demand opening in diseases hallmarked by dysfunction in pressure homeostasis (e.g. Glaucoma [34], intracranial hypertension [35]).

4. Conclusions

We have successfully demonstrated that mechanosensitive ion channel protein derived from multiple microbes is functional in mammalian cells, and the cells expressing SAM act as osmoregulatory and respond to physiological (osmotic shock) stress as measured by electrophysiology. Further, mutations to the residues of the mechanosensitive channel were found to adjust mechanosensitivity, including channel current and ion channel activity measured by dye intake. These results strongly suggest that the microbial channel (s) would function in the foreign environment under a specific range of mechanical stimuli or osmotic stress generated inside the body or externally using a specific device. Utilization of mechanosensitive channels of large conductance as a transgenic pressure modulator and alternative outflow actuator will enable the treatment of pressure-abnormality-related diseases involving cells susceptible to mechanical or osmotic stress.

5. Methods

5.1. Cloning of SAM variants

SAM variants (homologs and mutants) were synthesized and evaluated for membrane expression in mammalian cells, each SAM gene sequence was codon optimized for mammalian expression before synthesis. Genes were inserted into a pAAV-MCS vector backbone. The genes were put under the control of the CAG promoter. A fused fluorescent reporter (mCherry) was chosen to act as a visual marker of gene expression and membrane localization.

5.2. Cell culture

HEK 293 cells (ATCC, catalogue number: CRL-1573™, Research resource identifier: CVCL_0045) were grown in flasks in 1.5 mL of Dulbecco's modified Eagle's medium (DMEM) with 4.5 g/L glucose, L-glutamine and sodium pyruvate, 10% fetal bovine serum, 100 U/mL penicillin, and 100 μg/mL streptomycin sulfate and incubated in a humidified 5% CO_2 environment at 37 °C. A day before transfection, cells were plated in 35 mm Petri dishes in 1.5 ml of media and incubated at 37 °C until ~80% confluency.

5.3. Transfection

jetPRIME (Polyplus Transfection) was used to deliver ~2 μg of SAM-mCherry plasmid DNA to each dish. The plasmid DNA was added to 200 μl of jetPRIME buffer and then vortexed for 10 s. Then, 8 μl of jetPRIME was added, and the solution was left to sit at room temperature for 10 min. The solution was then added to the cells, and the sample was incubated at 37 °C for 2 h. The growth medium was exchanged for fresh media and incubated at 37 °C for another 48 h. At this time, fluorescence microscopy of live cells was used to confirm the successful transfection and expression of the fluorescent reporter (mCherry).

5.4. Assessment of cell viability

To determine the effect of SAM expression on the viability and functioning of cells in response to osmotic-stress conditions, measurements were carried out using a high throughput, automated fluorescence microscope (NucleoCounter® NC-3000™) with integrated data collection, analysis, and reporting. $N > 10^5$ cells were used for each of the SAM-transfected and -ve control groups.

5.5. Fluorescence confocal microscopy

Fluorescence Confocal Microscopy (Olympus Fluoview 1000) of live cells was used to confirm the successful transfection and expression of the fluorescent reporter-linked gene. The samples were excited at 543 nm, and a 560–660 nm red emission filter was used to visualize mCherry fluorescence.

5.6. Dye uptake assay

SAM variants act as an osmoregulator and gate in response to stretching of the cell membrane caused by turgor pressure. When the mechanosensitive ion channel opens, membrane-impermeable molecules can diffuse into and out of the cell through the open pore. Therefore, when subjected to a hypo-osmotic shock in the presence of extracellular membrane-impermeable molecules (including dyes or therapeutic agents), cells expressing functional SAM should uptake the molecule(s). HEK293 cells expressing SAM variants were subjected to a hypo-osmotic shock in the presence of ~2U/mL Alexa Fluor™ 488 Phalloidin (Invitrogen™) by the addition of 20–40% water (v/v). The cells were then monitored by confocal fluorescence microscopy (Olympus Fluoview 1000) for 15 min at 488 nm excitation and detected through a green emission filter (505–525 nm) for monitoring the dye. The fluorescence intensity in each cell was quantified longitudinally using ImageJ. For detecting mCherry, cells were excited by a 543 nm laser, and fluorescence was detected via a red emission filter (560–660 nm).

5.7. Functional characterization of SAM in mammalian cells using patch clamp electrophysiology

SAM channel function was probed by recording electrophysiological measurements from whole cell patches of HEK293 cells expressing SAM-mCherry. The patch-clamp recording setup includes an inverted Nikon fluorescence microscope (TS 100) platform using an amplifier system (Axon Multiclamp 700B, Molecular Devices) [36]. Micropipettes were pulled using a two-stage pipette puller (Narshinghe) to attain a resistance of 3–5 MΩ when filled with a solution containing (in mM) 130 K-Gluoconate, 7 KCl, 2 NaCl, 1 $MgCl_2$, 0.4 EGTA, 10 HEPES, 2 ATP-Mg, 0.3 GTP-Tris, and 20 sucrose. The micropipette-electrode was mounted on a micromanipulator. The extracellular solution contained (in mM): 150 NaCl, 10 Glucose, 5 KCl, 2 $CaCl_2$, and 1 $MgCl_2$ was buffered with 10 mM HEPES (pH 7.3). Inward currents were measured while holding cells in a voltage clamp at −70 mV. The electrophysiological signals from the amplifier were digitized using Digidata 1440 (Molecular Devices), interfaced with patch-clamp software (Clampex, Molecular Devices). A stable seal was achieved, and the current traces show channel activity only after the hypo-osmotic shock. Channel activity was induced by subjecting the patched cell to a hypo-osmotic shock by of 20% water (v/v).

For the automated pressure clamp, the Port-a-Patch system (Nanion, Germany) was used. Planar patch-clamp chips with a chip resistance of 2–3.5 MΩ were used. The internal solution consisted of 10 mM KCl, 10 mM NaCl, 110 mM K-Fluoride, 10 mM EGTA, 10 mM HEPES/KOH, and pH 7.2. The external solution consisted of 4 mM KCl, 140 mM NaCl, 1 mM $MgCl_2$, 2 mM $CaCl_2$, 5 mM D-Glucose monohydrate, and 10 mM HEPES/NaOH pH 7.4. The seal resistance was typically 1GΩ. The electrophysiological signals from the amplifier (Axon Multiclamp 700B, Molecular Devices) were digitized using Digidata 1440 (Molecular Devices). The pressure was introduced by Suction Control Pro (Nanion). The pClamp 10 software was used for data analysis.

5.8. Western blot analysis

Western blot experiments were performed to confirm the expression of the SAM protein by using an anti-mCherry antibody (NBP1-96752, Novus Biologicals). Briefly, cultured HEK293 cells were transfected with SAM plasmids by jetPRIME as described by the manufacturer. After 3 days of transfection, the cells were collected and then pelleted by centrifugation. The pellet was lysed in RIPA buffer (10 mM Tris-Cl [pH 8.0], 2 mM EDTA, 1% Triton X-100, 0.5% sodium deoxycholate, 0.1% SDS, and 150 mM NaCl) in the presence of protease inhibitor cocktail (Thermo Scientific). A clear supernatant for protein samples was collected after centrifugation at 14,000×*g* for 5 min. The total protein concentration was measured by a Pierce 660-nm protein assay (Thermo Fisher Scientific). The supernatant was transferred to an Eppendorf tube, and immunoprecipitation was performed using mouse anti-mCherry protein. The antibody/antigen complex was then pulled out using protein G-agarose beads (Pierce). The immunoprecipitated protein was separated by 4%–15% pre-made gradient gels (Bio-Rad), and proteins were transferred for 1 h at 120 V onto nitrocellulose membranes. Membranes were then blocked in skim milk for 60 min, followed by incubation with rabbit anti-SAM (LSBio Inc.), overnight at 4°C. Membranes were washed twice (15 min each) and then incubated with the secondary antibody, horseradish peroxidase-conjugated anti-rabbit immunoglobulin G (IgG) for 30 min (1:10,000; GE Healthcare). Membranes were washed three times (5 min each). The chemiluminescence was developed using a SuperSignal West Dura kit (Thermo Scientific) and the blot was imaged.

5.9. Statistics

Image processing and analysis were performed using NIH ImageJ software. GraphPad Prism was used to analyze the data. The data were plotted as mean ± S. D. Statistically significant difference analyses were carried out by *t*-test. $P < 0.05$ was considered statistically significant.

Data availability statement

The data generated and presented in this manuscript is available from the corresponding author upon reasonable request.

Ethics declarations

This study encompasses the results from in-vitro experiments only. Review and/or approval by an ethics committee is not applicable as it does not involve any animals or human subjects.

CRediT authorship contribution statement

Subrata Batabyal: Writing – review & editing, Writing – original draft, Methodology, Formal analysis. **Chinenye Idigo:** Methodology. **Darryl Narcisse:** Methodology. **Adnan Dibas:** Methodology, Conceptualization. **Samarendra Mohanty:** Writing – review & editing, Writing – original draft, Supervision, Conceptualization.

Declaration of competing interest

The authors declare that they have no known competing financial interests or personal relationships that could have appeared to influence the work reported in this paper.

Acknowledgments

The authors would like to thank Mr. Irtiza Ahmed (Nanoscope) for plasmid preparation and Dr. Kissaou Tchedre (Nanoscope) for help with Western blot.

Appendix A. Supplementary data

Supplementary data to this article can be found online at https://doi.org/10.1016/j.heliyon.2024.e29195.

References

[1] R.L. Gendron, E. Armstrong, H. Paradis, L. Haines, M. Desjardins, C.E. Short, W.R. Driedzic, Osmotic pressure-adaptive responses in the eye tissues of rainbow smelt (Osmerus mordax), Mol. Vis. 17 (2011) 2596–2604.
[2] C. Mangan, M.C. Stott, R. Dhanda, Renal physiology: blood flow, glomerular filtration and plasma clearance, Anaesth. Intensive Care Med. 19 (5) (2018) 254–257.
[3] C. Brocker, D.C. Thompson, V. Vasiliou, The role of hyperosmotic stress in inflammation and disease, Biomol. Concepts 3 (4) (2012) 345–364.
[4] N.I. Dmitrieva, L.F. Michea, G.M. Rocha, M.B. Burg, Cell cycle delay and apoptosis in response to osmotic stress, Comp. Biochem. Physiol. Mol. Integr. Physiol. 130 (3) (2001) 411–420.
[5] S.I. Sukharev, P. Blount, B. Martinac, F.R. Blattner, C. Kung, A large-conductance mechanosensitive channel in E. coli encoded by mscL alone, Nature 368 (6468) (1994) 265–268.
[6] C. Kung, B. Martinac, S. Sukharev, Mechanosensitive channels in microbes, Annu. Rev. Microbiol. 64 (2010) 313–329.
[7] A. Kloda, E. Petrov, G.R. Meyer, T. Nguyen, A.C. Hurst, L. Hool, B. Martinac, Mechanosensitive channel of large conductance, Int. J. Biochem. Cell Biol. 40 (2) (2008) 164–169.
[8] P. Wiggins, R. Phillips, Membrane-protein interactions in mechanosensitive channels, Biophys. J. 88 (2) (2005) 880–902.
[9] J. Ye, S. Tang, L. Meng, X. Li, X. Wen, S. Chen, H. Hu, Ultrasonic control of neural activity through activation of the mechanosensitive channel MscL, Nano Lett. 18 (7) (2018) 4148–4155.
[10] A. Soloperto, A. Boccaccio, A. Contestabile, M. Moroni, G.I. Hallinan, G. Palazzolo, F. Difato, Mechano-sensitization of mammalian neuronal networks through expression of the bacterial large-conductance mechanosensitive ion channel, J. Cell Sci. 131 (5) (2018) jcs210393.
[11] N. Levina, S. Tötemeyer, N.R. Stokes, P. Louis, M.A. Jones, I.R. Booth, Protection of Escherichia coli cells against extreme turgor by activation of MscS and MscL mechanosensitive channels: identification of genes required for MscS activity, EMBO J. 18 (7) (1999) 1730–1737.
[12] T.A. Walton, C.A. Idigo, N. Herrera, D.C. Rees, MscL: channeling membrane tension, Pflueg. Arch. Eur. J. Physiol. 467 (2015) 15–25.
[13] P. Blount, I. Iscla, Life with bacterial mechanosensitive channels, from discovery to physiology to pharmacological target, Microbiol. Mol. Biol. Rev. 84 (1) (2020), https://doi.org/10.1128/mmbr.00055-19.
[14] Z. Liu, C.S. Gandhi, D.C. Rees, Structure of a tetrameric MscL in an expanded intermediate state, Nature 461 (7260) (2009) 120–124.
[15] I.R. Booth, P. Blount, The MscS and MscL families of mechanosensitive channels act as microbial emergency release valves, J. Bacteriol. 194 (18) (2012) 4802–4809.
[16] E.S. Haswell, R. Phillips, D.C. Rees, Mechanosensitive channels: what can they do and how do they do it? Structure 19 (10) (2011) 1356–1369.
[17] D. Basu, E.S. Haswell, Plant mechanosensitive ion channels: an ocean of possibilities, Curr. Opin. Plant Biol. 40 (2017) 43–48.
[18] S. Amemiya, H. Toyoda, M. Kimura, H. Saito, H. Kobayashi, K. Ihara, Y. Nakashimada, The mechanosensitive channel YbdG from Escherichia coli has a role in adaptation to osmotic up-shock, J. Biol. Chem. 294 (33) (2019) 12281–12292.
[19] L.-M. Yang, D. Zhong, P. Blount, Chimeras reveal a single lipid-interface residue that controls MscL channel kinetics as well as mechanosensitivity, Cell Rep. 3 (2) (2013) 520–527.
[20] D. Zhong, P. Blount, Electrostatics at the membrane define MscL channel mechanosensitivity and kinetics, Faseb. J. 28 (12) (2014) 5234–5241.
[21] D. Zhong, P. Blount, Phosphatidylinositol is crucial for the mechanosensitivity of Mycobacterium tuberculosis MscL, Biochemistry 52 (32) (2013) 5415–5420.
[22] S.K. Mohanty, C.A. Idigo, Method, Compositions and Applications of Mechanosensitive Channels in Visual Disorders and Other Applications Thereof, Google Patents, 2023.

[23] Q. Xian, Z. Qiu, S. Murugappan, S. Kala, K.F. Wong, D. Li, M. Su, Modulation of deep neural circuits with sonogenetics, Proc. Natl. Acad. Sci. USA 120 (22) (2023) e2220575120.
[24] J.F. Doerner, S. Febvay, D.E. Clapham, Controlled delivery of bioactive molecules into live cells using the bacterial mechanosensitive channel MscL, Nat. Commun. 3 (1) (2012) 990.
[25] J. Heureaux, D. Chen, V.L. Murray, C.X. Deng, A.P. Liu, Activation of a bacterial mechanosensitive channel in mammalian cells by cytoskeletal stress, Cell. Mol. Bioeng. 7 (2014) 307–319.
[26] Z. Qiu, S. Kala, J. Guo, Q. Xian, J. Zhu, T. Zhu, H. Wang, Targeted neurostimulation in mouse brains with non-invasive ultrasound, Cell Rep. 32 (7) (2020).
[27] S. Cadoni, C. Demené, I. Alcala, M. Provansal, D. Nguyen, D. Nelidova, E. Burban, Ectopic expression of a mechanosensitive channel confers spatiotemporal resolution to ultrasound stimulations of neurons for visual restoration, Nat. Nanotechnol. 18 (6) (2023) 667–676.
[28] I.Y. Kuo, B.E. Ehrlich, Ion channels in renal disease, Chem. Rev. 112 (12) (2012) 6353–6372.
[29] V. Geraldes, S. Laranjo, I. Rocha, Hypothalamic ion channels in hypertension, Curr. Hypertens. Rep. 20 (2018) 1–11.
[30] S. Batabyal, Y.-T. Kim, S. Mohanty, Ultrafast laser-assisted spatially targeted optoporation into cortical axons and retinal cells in the eye, J. Biomed. Opt. 22 (6) (2017), 060504-060504.
[31] S. Batabyal, S. Gajjeraman, S. Bhattacharya, W. Wright, S. Mohanty, Nano-enhanced optical gene delivery to retinal degenerated mice, Curr. Gene Ther. 19 (5) (2019) 318–329.
[32] K. Dhakal, S. Batabyal, W. Wright, Y.-t. Kim, S. Mohanty, Optical delivery of multiple opsin-encoding genes leads to targeted expression and white-light activation, Light Sci. Appl. 4 (11) (2015) e352, e352.
[33] S. Batabyal, S. Gajjeraman, K. Tchedre, A. Dibas, W. Wright, S. Mohanty, Near-Infrared laser-based spatially targeted nano-enhanced optical delivery of therapeutic genes to degenerated retina, Mol. Therapy-Methods & Clin. Dev. 17 (2020) 758–770.
[34] M.B. Sultan, S.L. Mansberger, P.P. Lee, Understanding the importance of IOP variables in glaucoma: a systematic review, Surv. Ophthalmol. 54 (6) (2009) 643–662.
[35] B. Wakerley, M. Tan, E. Ting, Idiopathic intracranial hypertension, Cephalalgia 35 (3) (2015) 248–261.
[36] S. Batabyal, S. Gajjeraman, S. Pradhan, S. Bhattacharya, W. Wright, S. Mohanty, Sensitization of ON-bipolar cells with ambient light activatable multi-characteristic opsin rescues vision in mice, Gene Ther. 28 (3–4) (2021) 162–176.